

1 **Heat output by marine microbial and viral communities**

2

3 E. Djamali<sup>1,2</sup>, J. Nulton<sup>3</sup>, P. Turner<sup>1</sup>, F. Rohwer<sup>2</sup>, and P. Salamon<sup>3,\*</sup>

4

5 <sup>1</sup>Center for Hydrothermal Research, San Diego State University, San Diego, California  
6 92182-4614 USA

7

8 <sup>2</sup>Department of Biology, San Diego State University, San Diego, California 92182-4614  
9 USA

10

11 <sup>3</sup>Department of Mathematics & Statistics, San Diego State University, San Diego,  
12 California 92182-7720 USA

13

14 \* Corresponding author, salamon@sdsu.edu

15

16 Running Title: Heat from Pelagic Microbial Communities

17

18 Keywords: calorimetry, microbes, viruses, phage, pelagic, marine

19 Type of Article: manuscript

20 Number of words in summary: 197

21 Number of words in manuscript: 5724

22 Number of tables and figures: 8

23 Number of references: 21

24

24 **SUMMARY**

25           The Marine Microbial Food Web (MMFW) includes heterotrophic microbes and  
26 their protist and viral predators. These microbes consume dissolved organic matter  
27 thereby making the MMFW a major component of global biogeochemical and energy  
28 cycles. However, quantification of the MMFW contribution to these cycles is dependent  
29 on a handful of techniques, all of which require laboratory-derived conversion factors.  
30 Here we describe a differential calorimeter capable of measuring the small amounts of  
31 heat produced by MMFW microbes and viruses at natural concentrations. Using this  
32 ultrasensitive calorimeter, we show that heat production in the presence of viruses is  
33 significantly larger than in their absence. This increased heat output occurs despite a net  
34 decrease in the number of microbes. This provides direct evidence for top-down control  
35 of microbial populations by viruses and shows that there is increased remineralization. A  
36 comparative statics model was developed to interpret the calorimeter measurements. The  
37 model predicts that ~25% of the total heat production during the growth phase of a  
38 pelagic microbial community is due directly to viral activities. Together the model and  
39 calorimeter demonstrate a more direct way of measuring the work done by those  
40 components of the MMFW that are smaller than 0.45  $\mu\text{m}$ .

41

42

43

44

45

46

47 **1. INTRODUCTION**

48 Viruses are important marine microbial predators (Fuhrman, 1999; Wilhelm and  
49 Suttle, 1999; Wommack and Colwell, 2000; Wilhelm et al. 2002). In combination with  
50 protist grazing, viral predation is so intense that microbial numbers are maintained at  
51 values less than the carrying capacity of the system. This is called top-down control  
52 (Wilcox and Fuhrman, 1994; Sano et al. 2004) and has important implications for cycling  
53 rates of nutrients and energy in the world's oceans.

54 Dissolved organic matter (DOM) is the largest stock of biologically active carbon on the  
55 planet. DOM is essentially only consumed by heterotrophic microbes (both Bacteria and  
56 Archaea). Therefore, a major challenge to understanding global biogeochemical cycles, and  
57 particularly the carbon/energy budget, is quantifying the use of DOM by heterotrophic marine  
58 microbes. This has been a major methodological challenge since the discovery that there are ~0.5  
59 million microbes per milliliter of surface seawater. The main approach involves feeding microbes  
60 trace amounts of a radio(<sup>3</sup>H)- or chemical(Br-dUTP)-labeled metabolic intermediate (e.g., amino  
61 acids or thymidine) and then measuring incorporation into new microbial cells. This yields a  
62 measure of new cell production and energy usage is estimated using conversion factors derived  
63 from laboratory experiments (Fuhrman and Azam, 1982; Simon and Azam, 1989; Proctor and  
64 Fuhrman, 1990; Steward et al. 1992; Steward and Azam, 1999; Noble and Fuhrman, 2000).  
65 These conversion factors are the weak point in this approach and remain major topics of  
66 disagreement ever since their introduction. Other methods of measuring cell production include  
67 dilution experiments and direct counts. Again, conversion factors must be used to estimate energy  
68 expenditure. Changes in dissolved oxygen have also been used to measure microbial production.

69 These methods are limited by sensitivity and the fact that much of the MMFW metabolism may  
70 not use typical fixed carbon to oxygen respiration.

71 The measurement of heat from biochemical processes using a calorimeter offers a  
72 direct approach for monitoring microbial activities via their energy usage (Wadsö, 2002;  
73 Braissant et al., 2010). Calorimeters have been used to measure biological activity for more  
74 than two hundred years, but only in recent years has instrumentation become sufficiently  
75 sensitive to potentially perform such measurements on MMFW communities at natural  
76 densities. Due to limited sensitivity of available instrumentation, it has previously been  
77 necessary to artificially induce measurable amounts of heat production in these populations by  
78 compressing lab samples of pelagic microorganisms far beyond (100 times or more) their  
79 naturally-occurring densities (Pamatmat et al. 1981, Vandenhove et al. 1991, Gustafsson 1987,  
80 Larsson and Gustafsson 1999, Mukhanov et al. 2003, Mukhanov et al. 2004). This causes an  
81 observably significant disturbance to the microbial population. For example, one common  
82 approach to measuring heat from marine microorganisms has been to concentrate the  
83 population (Mukhanov et al. 2003, Mukhanov et al. 2004) by filtration and back-washing. This  
84 tends to compound the problem; marine microorganisms are typically non-culturable, and any  
85 significant disturbance to their natural environment can cause major changes in behavior. Thus  
86 it is desirable to conduct measurements without disturbing the natural environment, or at least  
87 by simulating that environment as closely as possible. Improved electronics design and  
88 computerized control practices have now made feasible calorimetry techniques to measure such  
89 natural or simulated communities.

90 Here we present the design of an isoperibol, temperature-rise, differential  
91 calorimeter capable of measuring open ocean marine microbial heat production at

92 concentrations of around  $10^5$  cells  $\text{ml}^{-1}$ . This calorimeter was used to measure the effects of  
93 viral predation on heat production. To interpret the measurements, a simple comparative-statics  
94 model was formulated. The results show that production-predation cycle in a simulated pelagic  
95 MMFW community decreases the total microbial cell count (net production) while increasing  
96 the total production (number of microbial replications).

97

## 98 **2. MATERIALS AND METHODS**

99

### 100 **2.1 Calorimeter design**

101 Calorimeters are commonly classified into two main types: isothermal, where the  
102 system is maintained at a fixed temperature by heat transfer to or from the surroundings, which  
103 thus provides a measure of the changes in the system; and adiabatic, where heat transfer  
104 between system and surroundings is prevented, so that the temperature change in the system  
105 provides the measure of heat. Neither strictly isothermal nor strictly adiabatic calorimeters are  
106 suited to measurement of the small heat changes involved in the pelagic systems considered  
107 here, because of the intrusive nature of the controls required to maintain the respective  
108 conditions. However, approximations to both types have the potential to achieve the desired  
109 results.

110 Currently, the heat conduction calorimeter (pseudo-isothermal) is the most common  
111 commercial type, in which heat is allowed to leak to or from the surroundings through a  
112 thermopile, which thus provides a direct electrical measure of the heat changes in the system  
113 (Braissant et al., 2010). However, isoperibol (pseudo-adiabatic) calorimeters, by which the  
114 system is insulated from isothermal surroundings and corrections are then applied for known

115 heat leakage, have the advantage of simplicity of construction. An isoperibol differential twin  
116 calorimeter, in which a reference system is placed inside the same isothermal enclosure as the  
117 measured system so that variations in heat leakage can be compensated continuously, has been  
118 constructed in our laboratory and appears to have sufficient sensitivity to monitor heat  
119 production from wild marine microbial communities at population densities typically found in  
120 pelagic environments ( $10^5$  cell/ml).

121         The calorimeter was constructed as follows. Reaction and reference glass vessels  
122 of approximately 25 ml capacity were placed in separate insulated Dewars within a 200-  
123 liter water bath. The water bath temperature was regulated with a thermostatic controller  
124 (Sargent-Welch Co., Model ST; Buffalo, New York) to give a temperature stability of  $\pm$   
125 0.005 °C. Thermistors (VEECO 0.100 glass probes series, 20 M $\Omega$ ) were used as the  
126 temperature-sensing elements and the reaction and reference vessel thermistors formed  
127 two arms of a Wheatstone bridge.

128         The long stems of the sample vessels are a press fit through the styrofoam  
129 stoppers of the Dewars, which basically act as internal air jackets (25 ml sample vessels  
130 in 500 ml Dewars). The Wheatstone bridge is driven by approximately 4 V batteries with  
131 the thermistors in series, so the power dissipation in both thermistors combined is on the  
132 order of 0.4  $\mu$ W. The thermistors were matched as closely as possible, and the difference  
133 in temperature change between sample and reference was small, so that self-heating was  
134 internally compensated by differential measurement. In 24 hours, error due to difference  
135 in self-heating is less than 0.1% of the total recorded output. Bridge current was  
136 approximately 100 nA. Thermistors were supplied sealed in glass; initially, we tried  
137 suspending them in contact with the sample but considerable electrical leakage was

138 found. Placing the thermistors in thin glass tubes with a little oil for thermal contact  
139 (NMR tubes worked well) seemed to eliminate the problem. Leads were bundled together  
140 and wrapped in Teflon tape to maximize compensation. The Dewars act as additional  
141 insulating air/vacuum jackets, and the sample vessels were assumed to be small enough  
142 that thermal conduction was adequate without stirring. It was also assumed that initial  
143 sample composition distribution was uniform. Temperature sensitivity of the bridge is  
144  $10^{-5}$  K. There was some bridge output amplification (normally  $10^3$ - $10^4$ ) using a Keithley  
145 155 microvoltmeter.

146 A personal computer was used for data collection and control via a 16-bit data  
147 acquisition board (Keithley, Inc., Model DAS-1802HR; Cleveland, Ohio). The  
148 calorimeter was provided with a calibration heater through which the chemical generation  
149 of heat by microbes was simulated by introducing a carefully measured quantity of  
150 electrical energy (Djamali et al 2010). A simplified diagram of the calorimeter is shown  
151 in Figure 1.

152 An electrical calibration heater ( $11 \Omega$ ) was made of glass-fiber insulated nickel-  
153 clad copper number 21 and a four-wire connection. This insulated electrical calibration  
154 heater was inserted into a glass well in the calorimeter through the lid of the vessel. For  
155 better thermal contact, the space between the electrical calibration heater and the well was  
156 filled with silicone oil. The calorimeter calibration heater is in the feedback of an  
157 operational amplifier (op-amp) and a standard resistor of  $10.00002 \Omega$  measures the  
158 current in the circuit, which is adjustable by the software. This introduces a precisely  
159 known amount of electrical energy into the system. Measurement of the voltage across  
160 this resistor gives the amount of current. The voltage across the heater is also measured.

161 The software can then continuously calculate the total energy introduced into the  
162 calorimetric system until this energy reaches a predetermined value. The circuitry for  
163 generating and measuring the electrical energy is described previously (Djamali et al.,  
164 2010). Electrical leakage to the thermistor was evident, but the bridge recovered in a few  
165 minutes and temperature rise appeared nearly vertical on the time scale of the experiment.

166 Heater power was 1-100 mW. Platinum thermometers were only used in the  
167 stirred outer bath, which was equipped with a control heater with power that was about  
168  $10^9$  times larger than the thermometer self-heating. Sample and reference containers and  
169 Dewars were switched with no apparent differences. Sample and reference vessels were  
170 80% filled, so there was an air space in the long and relatively narrow stem. The wiring  
171 was wrapped with Teflon tape to make a not-quite-airtight seal at the top of the stem to  
172 minimize evaporation.

173 The calorimeter was calibrated electrically. The overall accuracy of the  
174 measurements was approximately  $\pm 0.2$  %. From the electrical calibrations, the response  
175 time for a short burst of heat is on the order of 100 s; the response time for return to the  
176 original temperature is several days.

177 Experimental procedure for handling and introduction of sample into the  
178 calorimeter was revised in repeated experiments. Trial versions of the actual runs using  
179 blanks and with sterilized seawater in both sides, in absence of biological activity,  
180 produced no observable heat. Setting the initial state took 20 to 30 minutes.

181 In practice the A/D readings were output to a spreadsheet file, so essentially the  
182 temperature differences were logged in arbitrary temperature units; conversion to a  
183 standard temperature scale was done but is not strictly required. Conversion to heat

184 production was done by using the heat capacity calculated from the calibration runs. No  
185 significant correction for heat loss to the environment was required: in the absence of  
186 heat production in either vessel, the bridge output was essentially constant.

187         The absolute temperature of the calorimeter was determined by the use of a four–  
188 lead standard platinum resistance thermometer (Leeds and Northrup) and a Mueller  
189 Temperature Bridge (No. 8069). A platinum resistance element (Degussa Inc.) was  
190 calibrated against the platinum standard by mounting both of these elements in a metal  
191 block inside the stainless steel container (see Figure 1). Under equilibrium conditions the  
192 resistances of these two elements were compared and a calibration curve was constructed.  
193 The absolute temperature of the calorimeter vessel was determined by comparing the  
194 platinum resistance element with the calibration curve. In the calorimeter, the platinum  
195 resistance element was inserted in a metal block inside the Dewar flask (see Figure 1).

196

## 197 **2.2 Sample Preparation**

198         Seawater was collected off the pier at Scripps Institution of Oceanography (San Diego,  
199 CA) and placed in a 200-liter aquarium containing an assortment of macrofauna (corals, fish,  
200 and live rock), approximately 5 cm of crushed coral on the bottom, a protein skimmer, and  
201 carbon filter. The aquarium was outfitted with lighting, so both photosynthesis and respiration  
202 continued.

203         Three types of fractions were prepared from the aquarium samples by filtration  
204 using different pore sizes of a 50 mm diameter Sartorius membrane made of  
205 polyvinylidene fluoride: a sterile fraction, a viral fraction, and a microbe fraction referred  
206 to as the inoculum below. The smallest pore size (0.02  $\mu\text{m}$ ) allowed only dissolved

207 organic matter (DOM) to pass. This is the sterile fraction. The medium pore size (0.20  
208  $\mu\text{m}$ ) allowed the viral particles as well as some Eukaryotic virus to pass through along with  
209 the DOM. Finally, the coarse pore size (0.45  $\mu\text{m}$ ) allowed microbes, viruses and DOM to  
210 pass through. The sterile (DOM only) fractions were stored in a dark place and used as  
211 the dilution medium in the experiments. This is summarized in Figure 2. Prior to each  
212 experiment the sterile (DOM only) fraction was checked for microbial growth and if any  
213 growth was detected, the filtrate was discarded.

214         Levels of dissolved organic matter varied widely according to the feeding schedules of  
215 the macrofauna, so in order to compare biological activity in two samples it was necessary to  
216 collect pairs of samples simultaneously. Microbes from aquarium water samples, before and  
217 after each experiment, were directly counted using SYBR Gold. At least 20 fields were  
218 counted in each case. Cell counts are reported as the total number of microbial cells in  
219 each vessel. Reaction and reference vessel preparation protocols are summarized in the  
220 figures for each experiment. All the experiments were carried out at 23 °C.

221

### 222 **3. RESULTS AND DISCUSSION**

223         The goal of this work was to measure, by direct calorimetry, the effect of viruses  
224 on heat production in simulated pelagic communities. Calorimetric measurements are  
225 described which show that metabolic activity in the presence of viruses is more intensive  
226 than in their absence. Energy flows in viral:host interactions have been studied before by  
227 (Guosheng et al., 2003). Where comparable, our findings are in line with theirs, although  
228 our samples are pelagic communities at natural concentrations while Guosheng et al.  
229 study only the T4/*E. coli* system. The findings below have broad relevance; assessing the

230 extent of carbon cycling and energy release in pelagic microbial communities is of  
231 considerable interest in connection with global warming.

232

### 233 **3.1 The Four Experiments**

234 Recall that our goal is to compare the heat production from growing microbial  
235 communities with and without viral activity. Since our instrument is a *differential*  
236 calorimeter, i.e., one that measures the difference between the heat productions from two  
237 samples, we begin with a description of experiments in which one of the samples was  
238 sterile seawater. To facilitate the exposition, we will refer to four experiments, all but the  
239 last involving comparison with sterile seawater in one of the cells. These four  
240 experiments are illustrated in the four panels of Figure 3. In reality, variants of each of  
241 these 4 experiments were run many times, from different dilutions and using samples  
242 from the aquarium on different days.

243 As previously reported for near shore marine environments, (Wilcox and Fuhrman,  
244 1994; Sano et al. 2004) dilution of the community by 95% inhibits all lytic viral  
245 production. This matches our findings even up to 90% dilutions; 2 ml of inoculum added  
246 to 18 ml of sterile seawater (DOM) sample produced no measurable viral activity.

247 Each experiment started with a diluted microbial sample and ended with a  
248 stationary phase community producing very small amounts of heat. While the exact cause  
249 of this is not certain, the standard explanation of the onset of this phase is the depletion of  
250 nutrients, the buildup of toxins or possible quorum sensing among the microbes. The total  
251 heat production varied with the day sampling occurred. This implies that the total heat is  
252 probably limited by dissolved nutrient concentration, which varies over time according to

253 the aquarium maintenance schedule, rather than by dissolved oxygen content. It also  
254 indicates that meaningful comparison of infected and non-infected populations must be  
255 limited to samples collected at the same time. As discussed above, runs from different  
256 days were not directly comparable, although the inferred values of the heat associated  
257 with reproduction and lysis events were consistent between the runs.

258 The first three experiments compared reference cells with sterile seawater to  
259 reaction cells with various dilutions of inoculum: 95%, 90%, and 50%, respectively. The  
260 findings for the first two dilutions were consistent with the interpretation that there *is no*  
261 *viral activity at these dilutions* while the 50% dilution (experiment 3) resulted in very  
262 evident viral activity. The fourth and final experiment compared two samples with the  
263 viral fraction added in the ratio 17:3, one side of the calorimeter with intact viral particles  
264 and the other side with autoclaved viruses.

265

### 266 **3.2 Experiment 1: Microbial heat production without viruses**

267 Figure 4 shows an example of heat production for our first experiment. The  
268 calorimeter contained 20 ml of inoculum mixed with seawater (1ml:19ml) in the reaction  
269 vessel and an equal volume of sterile seawater, from the same source, in the reference  
270 vessel. The microbial cell count changed from  $4.6 \times 10^5$  to  $9.0 \times 10^6$  during the experiment.  
271 The temperature differences were rescaled to energy units using the heat capacities from  
272 the calibration runs. Microbial heat is generated in the reaction vessel, raising its  
273 temperature relative to the reference vessel; the difference levels off as nutrients are  
274 depleted (see discussion above). The temperature change during the experiment was  
275 approximately 0.005 °C. The power per microbial cell in these experiments, at the stage

276 where population approaches steady state, was in the range of (30 to 200) fW, consistent  
277 with the value previously reported (Mukhanov et. al. 2003). In a later investigation  
278 (Mukhanov et. al. 2004) it was concluded that the average power per microbial cell had  
279 an inverse relation with concentration of the microbes present and this is also consistent  
280 with our findings. In the present study, the concentration of microbial cells was 2 to 3  
281 orders of magnitude less per ml than the previous study (Mukhanov et. al. 2003). In the  
282 absence of viruses and presence of excess nutrients, the initial power output per microbial  
283 cell from this study was in the range of (30 to 90) pW cell<sup>-1</sup>.

284 The average heat per reproduction event for this experiment is  $0.42 \text{ J} / (9 \times 10^6 -$   
285  $0.5 \times 10^6) \text{ cells} \approx 50 \text{ nJ/cell}$ .

286

### 287 **3.3 Experiment 2: The effect of autoclaved DOM**

288 In order to illustrate the consistency of heats and to further validate the  
289 assumption that the viruses were sufficiently dilute in experiment 1 to suppress any viral  
290 activity, experiments were performed on aquarium water samples at various dilutions and  
291 using different DOM solution sterilization methods. In the second experiment, shown in  
292 Figure 5, the inoculum was only diluted to 90% (2ml added to 18 ml). No viral activity  
293 was detected in either of the two variants: one in which the DOM solution is autoclaved  
294 to ensure sterility while in the other sterility arises only as a result of the filtration. While  
295 the total heat produced was very nearly the same (0.63 J vs. 0.62 J), the autoclaved  
296 sample gave much less power initially, possibly due to structural changes in the nutrients  
297 causing slower metabolism without changing the total available energy.

298           The average heat per reproduction event for this experiment was  $0.62 \text{ J} / 14.7 \times 10^6$   
299 cells = 42 nJ/cell and  $0.63 \text{ J} / 12.6 \times 10^6$  cells  $\cong$  50 nJ/cell respectively.

300

### 301 **3.4 Experiment 3: Heat production with combined microbial and viral communities**

302           At sufficiently high dilutions, viruses are not able to infect their target microbes  
303 before they degrade. The first two experiments, shown in Figures 4 and 5, constitute a  
304 calibration where the heat production is essentially all due to microbial growth. In the  
305 third experiment, to assure that viral activity would be present, the dilution was decreased  
306 to 50%, again using a sterile reference sample. The measured heat is shown in Figure 6.  
307 The average heat per reproduction event for this experiment is masked by the viral  
308 activity but if one repeats the naïve calculation carried out above, the mean heat per unit  
309 increase in microbial count is  $0.48 \text{ J} / 1.3 \times 10^6$  cells  $\cong$  370 nJ/cell. This additional heat is  
310 accounted for more carefully after the discussion of a comparative-statics model  
311 presented in section 4.

312

### 313 **3.5 Experiment 4: Heat production with intact and autoclaved viruses**

314           For our final experiment shown in Figure 7, the reference and the reaction cells  
315 both contained mixtures of all three fractions, the difference being that the viral fraction  
316 was sterilized in the autoclave for the reference samples but not for the reaction samples.  
317 The three runs shown differ in the initial viral concentrations and show, in agreement with  
318 Mukhanov et. al. (2004), that the more dilute the solution the higher the difference in the  
319 amount of heat produced. The side with live viruses always produced significantly more  
320 heat and resulted in lower final microbial counts than the side with the autoclaved viruses.

321 We postpone a quantitative discussion of these three runs until after a presentation of the  
322 comparative statics model in the next section.

323

## 324 **4. ACCOUNTING FOR HEAT PRODUCTION BY MICROBES IN THE** 325 **PRESENCE OF VIRUSES**

326

### 327 **4.1. Background**

328 Two biological sources of heat were considered: (1) microbial growth and  
329 replication, and (2) viral replication and subsequent lysis of the host. The average heat  
330 from growth and cell division leading to the formation of one new microbial cell (a  
331 replication event) is approximately constant for the pelagic communities measured. This  
332 heat was directly available in the first two experiments. As discussed above, the samples  
333 varied greatly with the extent of dilution, times of cleaning the tank and the addition of  
334 nutrients. There was no consistency in the levels of microbes before and after the runs or  
335 in the total amount of heat produced. Nonetheless, the total heat produced divided by the  
336 increase in the number of microbes in all the runs with negligible viral activity were  
337 constant and approximately 50 nJ.

338 The heat produced during the destruction of a single microbial cell by viral  
339 replication and enzymatic lysis is more elusive. Given our findings that the average heat  
340 of a microbial reproduction event is constant, it is reasonable to assume that such lysis  
341 events also have a constant associated average heat. The model below enables one to  
342 count the number of lytic events based only on the initial and final microbial counts and  
343 the net difference in heat produced. The central variable in this model is the ratio  $r$  of the

344 heat in one lytic event to the heat in one reproduction event. We strive to keep all the  
345 modeling at the simplest level and thus stick to the net changes observed in each  
346 experiment. In particular, *we make no attempt to model the dynamics of the complex*  
347 *communities in our samples*, as we believe such modeling to lie well beyond the scope of  
348 this paper. Rather we focus on the net changes in the experiments that present food to an  
349 initially stationary phase microbial population and follow the heat evolved and microbes  
350 produced in this population until it reaches stationary phase once again. Our thesis below  
351 is that such net changes can be simply and consistently interpreted.

352 Let  $q^+$  represent the average heat associated with one replication event and  $q^-$   
353 represent the average heat associated with one lytic event. The crucial unknown is the  
354 ratio  $r=q^-/q^+$  of the heat per *lytic* event divided by the heat per *reproduction* event. For  
355 the T4/*E-coli* system studied by Guosheng et. al., the reported values lead to this ratio  
356 equaling 0.78 (see p. 141 in Guosheng et. al., 2003).

357 Quite generally, this ratio is expected to be on the order of one, probably between  
358 one half and one. Evolutionary forces select for viruses that optimally use up their hosts  
359 and thus recycle most of the material within the microbial cell. Micrographs of microbes  
360 crowding with viral particles add credence to this expectation. On thermodynamic  
361 grounds, one would expect a comparable amount of irreversible heat production from the  
362 salvage operations carried out by virus on a microbe to the heat produced during the  
363 construction of that microbe. Most of the biosynthesis required for microbial and viral  
364 growth does not require complete chemical dismantling of nutrient monomers. For  
365 example, it is possible in-principle to construct the DNA of one species simply by  
366 rearranging the nucleotides from the DNA of another species. The heat of reaction for

367 this rearrangement is about zero although the biosynthesis still requires ATP. While the  
368 net heat of the reaction is zero, the spontaneity of the reactions requires that some free  
369 energy be degraded to heat. The oxidation of nutrients to generate ATP is exothermic and  
370 usually much larger than the average heat of formation of one biopolymer from another.  
371 Since the virus is actually using the metabolic system of the microbe, biochemical  
372 strategies and associated heat production are likely to be similar for microbial and viral  
373 growth.

374

#### 375 **4.2. The Calculations**

376 Let  $N^+$  represent the number of microbial replication events during the experiment  
377 and  $N^-$  the number of lysis events. The total heat produced is

$$378 \quad Q^{\text{tot}} = q^+ N^+ + q^- N^- \quad (1)$$

379 with an associated net change in microbial population of

$$380 \quad \Delta N = N^+ - N^- . \quad (2)$$

381 Note that this net change in the number of microbes is given as all “births” minus all  
382 “deaths”. Given the measured values of  $Q^{\text{tot}}$  and  $\Delta N$  for a cell and an assumed value of  $r$ ,  
383 equations 1 and 2 determine the values of the number of reproduction events,  $N^+$ , and the  
384 number of lytic events,  $N^-$ , in that cell.

385

#### 386 **4.2a. Experiments 1 and 2.**

387 In the first two experiments (Figures 4 and 5), the reference cell contained sterile  
388 seawater and so produced no heat and no microbes. The reaction vessel was inoculated  
389 with aquarium water at a dilution level sufficient to render any virus harmless.

390 Consequently, in these experiments, the production of heat can be attributed exclusively  
 391 to microbial growth. That is,  $N^- = 0$  in equations 1 and 2, while  $\Delta N$  and  $Q^{\text{tot}} = Q^{\text{meas}}$  are  
 392 measured directly as the change in cell count and the total differential heat produced.  
 393 Thus these experiments can give calculated values of the average heat of one  
 394 reproduction event

$$395 \quad q^+ = Q^{\text{tot}}/N^+ = Q^{\text{meas}}/\Delta N. \quad (3)$$

396 The values of  $q^+$  calculated from the data shown in Figures 4 and 5 are  $q^+ = 50, 42,$  and  
 397  $50 \text{ nJ cell}^{-1}$  respectively. For the subsequent analysis of experiments 3 and 4 (Figures 6  
 398 and 7) the value of  $q^+$  is taken as  $50 \text{ nJ cell}^{-1}$ .

399

#### 400 **4.2b. Experiment 3**

401 In the third experiment (Figure 6), the dilution of the inoculum was 50%,  
 402 resulting in considerable viral activity in the reaction vessel. Since the reference cell had no  
 403 microbes present, we may again identify  $Q^{\text{meas}} = Q^{\text{tot}} = 0.48 \text{ J}$ . This total heat can then be  
 404 used to determine  $(N^+ + rN^-) = Q^{\text{tot}}/q^+ = 9.6 \cdot 10^6$  cells using equation (2) while the  
 405 measured change in cell count,  $\Delta N = 1.3 \times 10^6$  cells determines  $(N^+ - N^-)$ . The values of  
 406  $N^+$  and  $N^-$  can then be determined by solving these two linear equations in two unknowns,  
 407 giving

$$408 \quad \begin{aligned} N^+ &= \frac{10^7 + 1.3 \cdot 10^6 r}{1 + r} \\ N^- &= \frac{8.7 \cdot 10^6}{1 + r} \end{aligned} \quad (4)$$

409

410 For  $r=1$ , we find  $N^+ = 5.65 \times 10^6$  cells and  $N^- = 4.35 \times 10^6$  cells. For  $r = 0.5$ , we find  $N^+ =$   
 411  $7.1 \times 10^6$  cells and  $N^- = 5.8 \times 10^6$  cells. As discussed above, the true values are expected to  
 412 be somewhere in between. Note that to one significant figure the number of replication  
 413 events  $N^+$  is in either case about five times the net observed increase of  $\Delta N = 1.3 \times 10^6$   
 414 cells.

415

#### 416 **4.2c. Experiment 4**

417 The fourth experiment (Figure 7) compared microbial activity with and without  
 418 viruses. Microbes were delivered to both reaction and reference vessels in the form of a  
 419 5% inoculum, by itself dilute enough to suppress viral activity. Viruses were introduced  
 420 separately into the reaction vessel in a concentrated form to guarantee the presence of  
 421 viral particles in excess. In this case, since the reference vessel contains growing  
 422 microbes, the determination of  $N^+$  and  $N^-$  is slightly more involved.

423 The heat produced in the *reference* cell (with no viral activity) is calculated as

$$424 \quad Q_{ref}^{tot} = q^+ \Delta N_{ref} \quad (5)$$

425 and the heat produced in the reaction vessel as

$$426 \quad Q_{rxn}^{tot} = Q^{meas} + Q_{ref}^{tot} . \quad (6)$$

427 Combining this with the observed  $\Delta N_{rxn}$  enables us to determine  $N_{rxn}^+$  and  $N_{rxn}^-$  using  
 428 equations 1 and 2.

429 As an example, consider the red curve in Figure 7. The change in the cell counts  
 430 in the reference vessel is

$$431 \quad \Delta N_{ref} = 22.8 \times 10^6 - 0.1 \times 10^6 = 22.7 \times 10^6 \text{ cells} \quad (7)$$

432 giving

433 
$$Q_{ref}^{tot} = 50nJ \times 22.7 \times 10^6 = 1.13J. \quad (8)$$

434 This then determines the total heat from the reaction side as

435 
$$Q_{rxn}^{tot} = Q^{meas} + Q_{ref}^{tot} = 1.37J + 1.13J = 2.5J \quad (9)$$

436 using equation 6. Utilizing equation 9, equation 1 rearranges to

437 
$$N_{rxn}^+ + rN_{rxn}^- = \frac{2.5J}{q^+} = 50 \times 10^6 \text{ cells.} \quad (10)$$

438 Combining this with the net change in cell counts for the reaction vessel

439 
$$N_{rxn}^+ - N_{rxn}^- = 16.7 \times 10^6 - 0.1 \times 10^6 = 16.6 \times 10^6 \text{ cells} \quad (11)$$

440 gives

441 
$$N^+ = \frac{5 \cdot 10^7 + 1.66 \cdot 10^7 r}{1 + r} \quad (12)$$

442 
$$N^- = \frac{3.3 \cdot 10^7}{1 + r}$$

442

443 For  $r=1$  these become  $N_{rxn}^+ = 33.3 \times 10^6$  cells and  $N_{rxn}^- = 16.7 \times 10^6$  cells. For  $r=0.5$  these

444 become  $N_{rxn}^+ = 38.8 \times 10^6$  cells and  $N_{rxn}^- = 22.2 \times 10^6$  cells. The calculations for the other

445 initial concentrations proceed in the same way; the results are summarized in Table 1.

446

### 447 **4.3 Fraction of heat attributable to viral activity**

448 In this section we decompose the total heat released in one cell into three parts.

449 The first part is the heat *directly* attributable to viral activity,  $Q_{phage}^{dir} = q^- N^-$ . The second

450 part is the heat *indirectly* attributable to viral activity  $Q_{phage}^{indir} = q^+ N^-$ . This is the heat

451 produced by the microbes in effectively producing food for the viruses. The final part

452  $Q_{prod} = q^+ \Delta N$  is the heat associated with net microbe production. Note that these three

453 terms add up to the total heat  $Q^{tot} = q^+N^+ + q^-N^- = q^+\Delta N + q^+N^- + q^-N^-$ . The fraction of  
 454 heat directly or indirectly attributable to viruses

$$455 \quad \alpha = \frac{Q_{phage}^{dir} + Q_{phage}^{indir}}{Q_{tot}} = \frac{Q_{phage}^{tot}}{Q_{tot}} = \frac{q^+N^- + q^-N^-}{q^+N^+ + q^-N^-} = 1 - \frac{q^+\Delta N}{Q_{tot}} \quad (13)$$

456 ranges between 0.44 and 0.88 in the experiments presented. Note that its value is  
 457 independent of the value of  $r$  as can be seen from the last expression in equation 13. The  
 458 fraction of heat directly attributable to viral activity

$$459 \quad \beta = \frac{Q_{phage}^{dir}}{Q_{tot}} = \frac{q^-N^-}{q^+N^+ + q^-N^-} \quad (14)$$

460 does show an  $r$  dependence. The dependence of  $\beta$  on  $r$  is fairly simple however.

$$461 \quad \beta(r) = \left( \frac{2r}{1+r} \right) \cdot \beta(1) \quad (15)$$

462 where  $\beta(1) = \alpha/2$  is the fraction of heat directly attributable to viruses assuming  $r = 1$ . As  
 463 seen in Table 1, assuming  $r = 0.5$ , results in  $\beta$  values that range from 0.15 to 0.29, while  
 464 assuming  $r = 1.0$ , results in  $\beta$  values that range from 0.22 to 0.44.

465

## 466 5. CONCLUSIONS

467

468 The present paper reports calorimetric measurements of marine microbes smaller  
 469 than  $0.45 \mu\text{m}$  at pelagic concentration, albeit from an aquarium. The goal was to  
 470 demonstrate a calorimetric method for assessing what fraction of the heat produced in a  
 471 microbial community is due to viral activity.

472 The measurements showed that in the presence of viruses, the total heat  
 473 production is increased, while the final microbial cell count is decreased. Microbes

474 apparently reproduce faster in the presence of viruses. This has been observed by other  
475 investigators for the T4-*E. coli* system (Guosheng et al., 2003). The likely explanation is  
476 that viral lysis creates DOM accessible to other microbes (Middelboe et al. 2003). The  
477 final microbial count being decreased in the presence of live viral particles is evidence for  
478 top-down control of the microbial population.

479         The apparatus described here makes it possible to perform calorimetric  
480 measurements on intact pelagic microbial communities. Furthermore, this design could  
481 be adapted to a portable "nanocalorimeter" which could be deployed in the field to  
482 measure microbial heat production in natural environments.

483         The heat production in all our experiments leveled off to a steady state when the  
484 nutrient supply ran out. Our measurements for the heat produced in such steady states are  
485 in close agreement with (Mukhanov et. al., 2003). Surprisingly the heat production per  
486 microbe increased with dilution contrary to what was naively expected but in line with  
487 the results of (Mukhanov et. al., 2004) who reported an inverse proportionality between  
488 heat production and microbial concentration.

489         A simple comparative-statics model was introduced to account for the heat  
490 production in the presence of virus activity. The model infers the number of lytic events  
491 from the excess heat production. To within a factor of two, the fraction of heat directly  
492 attributable to chemistry carried out by viruses is about 0.3 while the fraction of heat  
493 directly or indirectly attributable to viral activity is about 0.7. This makes viruses major  
494 players in the energy budget for our planet and has important implications for carbon  
495 cycling.

496

497 **6. ACKNOWLEDGEMENTS**

498

499           We are grateful to Richard B. Kemp for reading a preliminary version of the  
500 manuscript and for arranging invaluable feedback on its contents from several  
501 anonymous readers.

502

503

504

505

506

507

508

509

510

511

512

513

514

515

516

517

517 **7. REFERENCES**

518

519 Braissant, O; Wirz, D; Göpfert, B. & Daniels, A.U. (2010) Use of isothermal  
520 microcalorimetry to monitor microbial activities *FEMS Microbiol Lett* **303**: 1–8.

521 Djamali, E., Turner, P.J., Murray, R.C. & Cobble, J.W. (2010) A High-Temperature  
522 High-Pressure Calorimeter for Determining Heats of Solution up to 623 K *Rev.*  
523 *Sci. Instrum.* **81**: 075105.

524 Fuhrman, J. A. and Azam, F. (1982) Thymidine incorporation as a measure of  
525 heterotrophic bacterioplankton production in marine surface waters: Evaluation  
526 and field results. *Journal Marine Biology.* **66**: 1432-1793.

527 Fuhrman, J. A. (1999) Marine viruses: biogeochemical and ecological effects. *Nature*  
528 **399**: 541–548.

529 Guosheng, L., Yi, L., Xiangdong, C., Peng, L., Ping, S., Songsheng, Q. (2003) *J. Virol.*  
530 *Methods* **112**:137-143.

531 Gustafsson, L. (1987) Microcalorimetry as a tool in microbiology and microbial ecology.  
532 In *Microbes in the Sea*, Sleigh, M.A., (Ed.), Chichester: Ellis Horwood Ltd., p  
533 167.

534 Larsson, B., and Gustafsson, L., (1999) Calorimetry of Microbial Processes. In *Handbook*  
535 *of Thermal Analysis and Calorimetry*, Kemp, R.B. (Ed.), Vol. 4, Amsterdam:  
536 Elsevier, p 390.

537 Middelboe, M., Riemann, L., Steward, G.F., Hansen, V., Nybroe, O. (2003) Virus-  
538 induced transfer of organic carbon between marine bacteria in a model  
539 community. *Aquatic Microbial Ecology* **33**:1-10.

540 Mukhanov, V., Rylkova, O., Lopukhina, O., Kemp, R.B. (2003) Productivity and  
541 thermodynamics of marine bacterioplankton: an inter-ecosystem comparison.  
542 *Thermochim. Acta*, **397**: 31-35.

543 Mukhanov, V.S., Naidanova, O.G., Shadrin, N.V., and Kemp, R.B., (2004) The spring  
544 energy budget of the algal mat community in a Crimean hypersaline lake  
545 determined by microcalorimetry. *Aquat. Ecol.*, **38**: 375-385.

546 Noble, R. T., and Fuhrman, J. A. (2000) Rapid virus production and removal as measured  
547 with fluorescently labeled viruses as tracers. *Appl. Environ. Microbiol.* **66**: 3790–  
548 3797.

549 Pamatmat, M. M., Graf, G., Bengtsson, W., and Novak, C. S. (1981) Heat production,  
550 ATP concentration and electron transport activity of marine sediments. *Mar. Ecol.*  
551 *Progr. Ser.* **4**: 135.

552 Proctor, L. M., and Fuhrman, J. A. (1990) Viral mortality of marine bacteria and  
553 cyanobacteria. *Nature* **343**: 60–62.

554 Sano E., Carlson S., Wegley L., and Rohwer F. (2004) Movement of viruses between  
555 biomes. *Appl Environ Microbiol.* **70**:5842-6.

556 Simon, M., Azam, F. (1989) Protein content and protein synthesis rates of planktonic  
557 marine bacteria. *Marine Ecology Progress Series.* **51**: 201-213.

558 Steward, G. F., Wikner, J., Smith, D. C., Cochlan, W. P., and Azam, F. (1992) Estimation  
559 of virus production in the sea: I. Method development. *Mar. Microb. Food Webs*  
560 **6**: 57–78.

561 Steward, G. F., Azam, F. (1999) Bromodeoxyuridine as an alternative to 3H-thymidine  
562 for measuring bacterial productivity in aquatic samples. *Aquatic Microbial*  
563 *Ecology*. **19**: 57-66.

564 Vandenhove, H., Merckx, R., Wilmots, H., and Vlassak, K., (1991) Survival of  
565 *Pseudomonas fluorescens* inocula of different physiological stages in soil. *Soil*  
566 *Biol. Biochem.* **23**: 1133.

567 Wadsö, I (2002) Isothermal microcalorimetry in applied biology *Thermochimica Acta*  
568 **394**: 305–311.

569 Wilcox, R. M., and Fuhrman, J. A. (1994) Bacterial viruses in coastal seawater: lytic  
570 rather than lysogenic production. *Mar. Ecol. Prog. Ser.* **114**: 35–45.

571 Wilhelm, S. W., and Suttle, C. A. (1999) Viruses and nutrient cycles in the sea play  
572 critical roles in the structure and function of aquatic food webs. *Bioscience* **49**:  
573 781–788.

574 Wilhelm, S. W., Brigden, S. M., and Suttle, C. A. (2002) A dilution technique for the  
575 direct measurement of viral production: a comparison in stratified and tidally  
576 mixed coastal waters. *Microb. Ecol.* **43**: 168–173.

577 Wommack, K. E., and Colwell, R. R. (2000) Virioplankton: viruses in aquatic  
578 ecosystems. *Microbiol. Mol. Biol. Rev.* **64**: 69–114.

579

580

581

582

583

584

Experiment #	WITHOUT PHAGE ACTIVITY			WITH PHAGE ACTIVITY			
	1	2 (red)	2 (black)	3	4 (red)	4 (blue)	4 (black)
$Q^{\text{meas}}$ (J)	0.43	0.62	0.63	0.5	1.37	0.63	0.44
$\Delta N_{\text{rxn}}$	8.54	14.67	12.61	1.3	16.6	5.2	16.6
$\Delta N_{\text{ref}}$	0	0	0	0	22.7	8.4	20.5
$q$ (nJ)	0.05	0.042	0.05	0.05	0.05	0.05	0.05
$Q_{\text{rxn}}^{\text{tot}}$ (J)	0.43	0.62	0.63	0.5	2.5	1.06	1.46
$Q_{\text{ref}}^{\text{tot}}$ (J)	0	0	0	0	1.135	0.42	1.02
$N_{\text{rxn}}^+$	8.54	14.67	12.61	5.65	33.35	13.2	22.95
$N_{\text{rxn}}^-$	0	0	0	4.35	16.75	8	6.35
$\alpha$	0	0	0	0.88	0.66	0.76	0.44
$\beta, r=0.5-1$	0	0	0	0.29-0.44	0.22-0.33	0.25-0.38	0.15-0.22

585

586 Table 1. Calculated quantities for analyzing microbial energy use and viral activity  
 587 indices in the four experiments. The last row lists ranges of  $\beta$  values corresponding to the  
 588 assumptions of  $r = 0.5$  and  $r = 1.0$ .

589

590

591

592

593

594

595

596

597

598

599

600 FIGURE CAPTIONS

601

602 Figure 1. (A) Simplified Diagram of the Differential Calorimeter. (B) Reaction and  
603 Reference Vessel.

604

605 Figure 2. Calorimetric Sample Preparation. Aquarium water was separated into three  
606 fractions by filtration. These fractions were used to mix the contents of the reference and  
607 reaction cells in the calorimeter.

608

609 Figure 3. Mixtures of the filtrates used in the reference and the reaction cells in the four  
610 experiments.

611

612 Figure 4. Differential heat output vs. time comparing sterile seawater and seawater with  
613 inoculum diluted 95%. At this dilution, no viral lysis takes place. The heat produced per  
614 unit increase in microbial count is 50 nJ.

615

616 Figure 5. Differential heat output vs. time comparing sterile seawater and seawater with  
617 inoculum diluted 90%. Also at this dilution, no viral lysis takes place. The two curves  
618 compare the heat evolution vs. time from aquarium water samples with seawater  
619 sterilized by filtration only and seawater sterilized by autoclaving. The heat produced per  
620 unit increase in microbial count is 42nJ and 50 nJ for the two runs.

621

622 Figure 6. Differential heat output vs. time comparing sterile seawater and seawater with  
623 inoculum diluted 50%. At this concentration the viruses are active. The heat produced per  
624 unit increase in microbial count is 370 nJ.

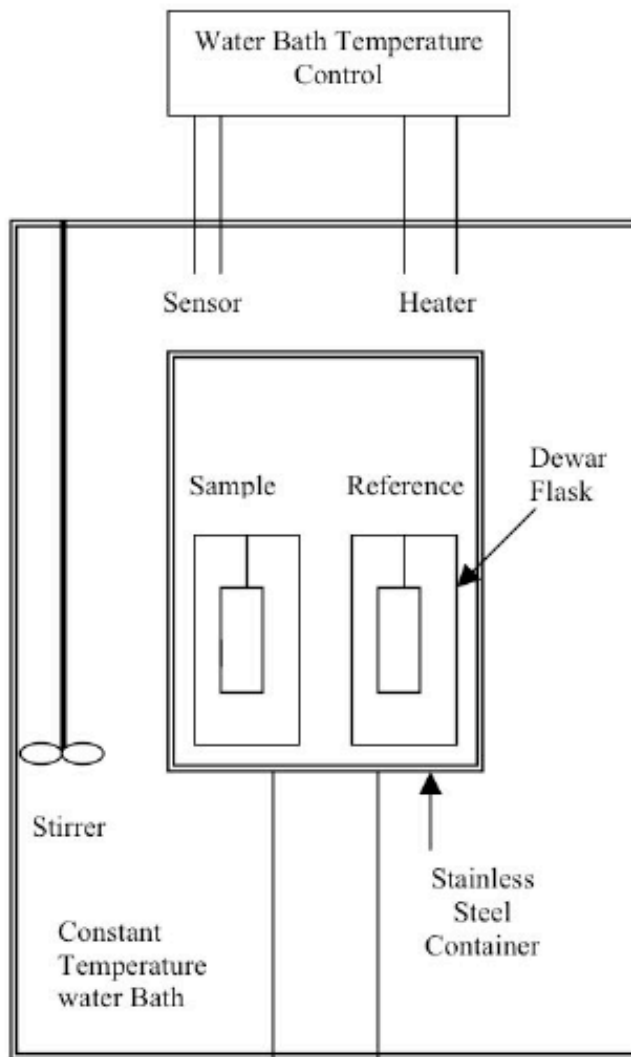
625

626 Figure 7. Differential heat output vs. time comparing microbial heat production in the  
627 presence of concentrated live and autoclaved viruses. Measurements from three different  
628 initial counts of inoculum are shown:  $0.1 \times 10^6$  (red),  $0.4 \times 10^6$  (blue) and  $0.9 \times 10^6$  (black)  
629 microbes. This time heat is produced in both the reference and in the reaction cell. The  
630 analysis is presented in sections 4.2c. The results of the calculations are shown in Table  
631 1.

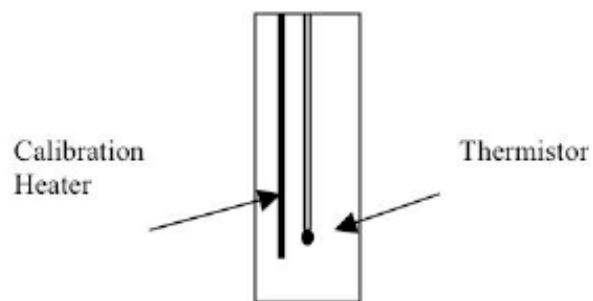
632

633

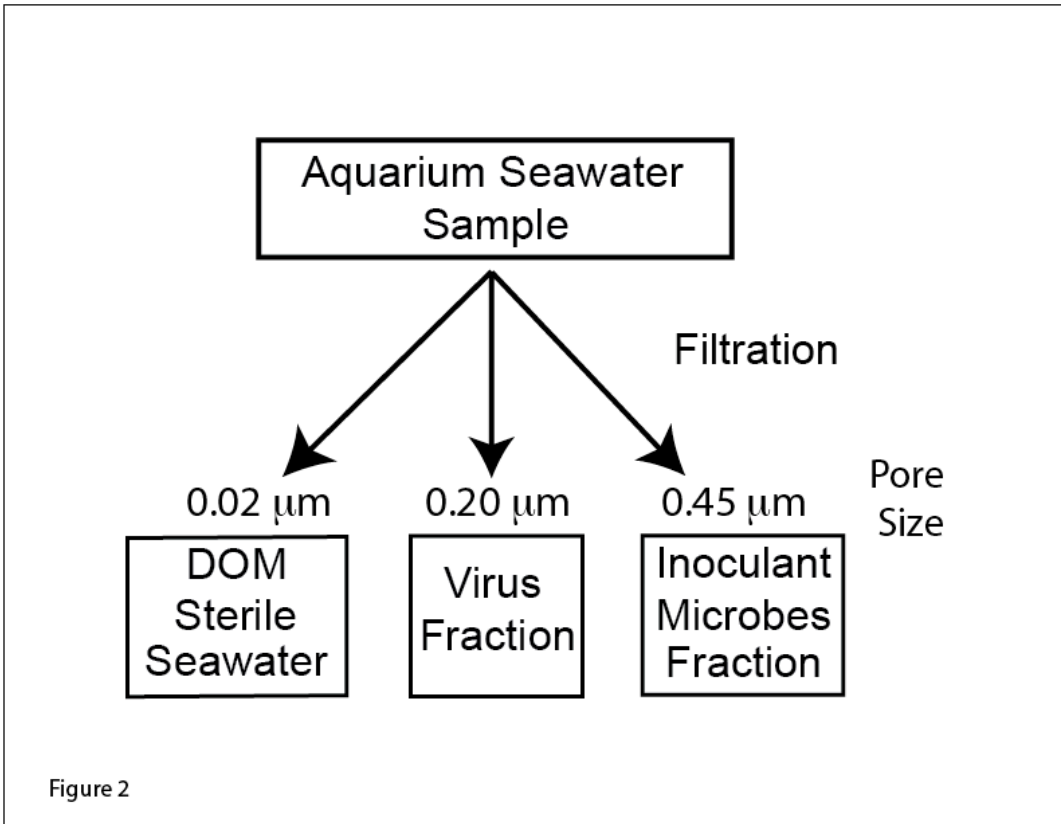
634



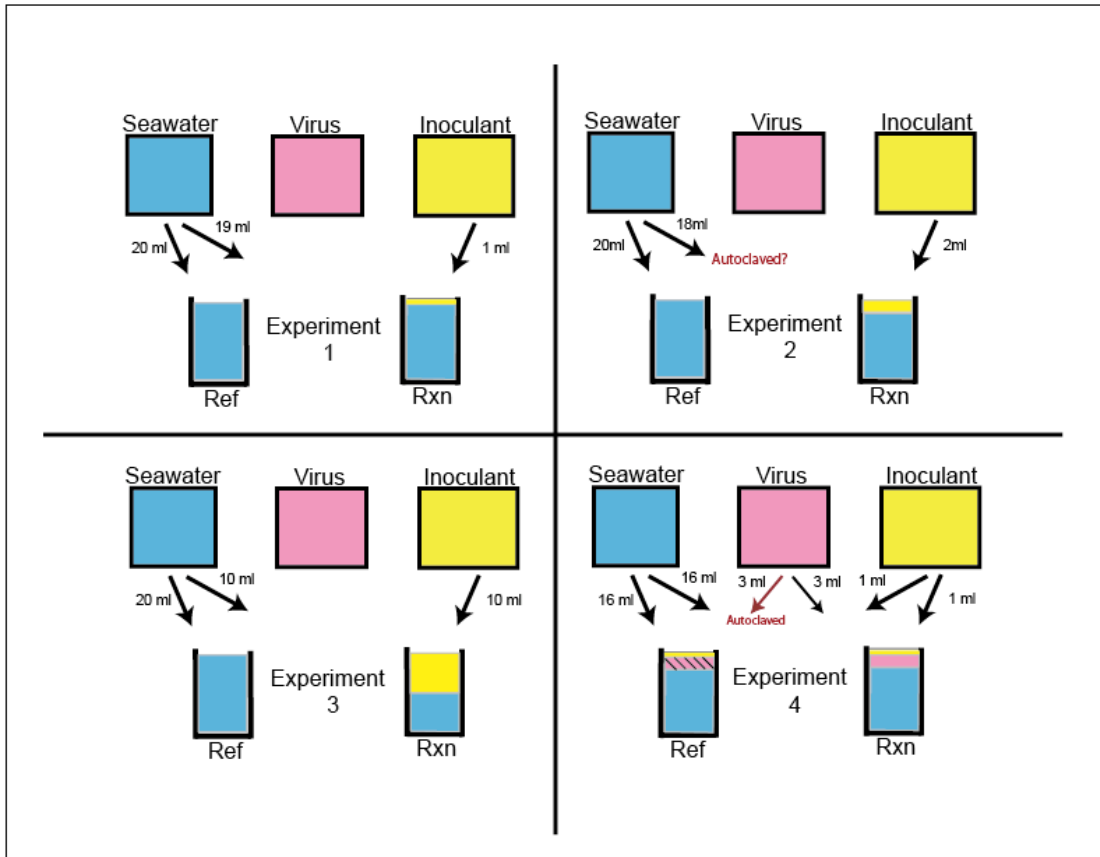
A. Calorimeter.



634  
 635 Fig 1  
 636

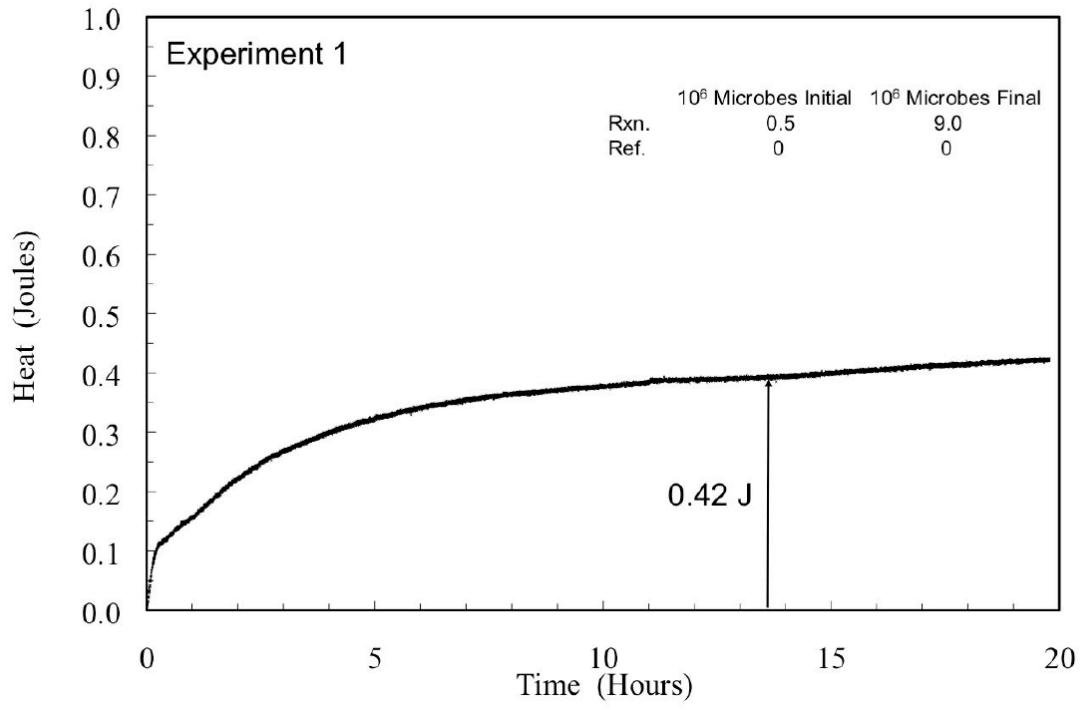


636  
637

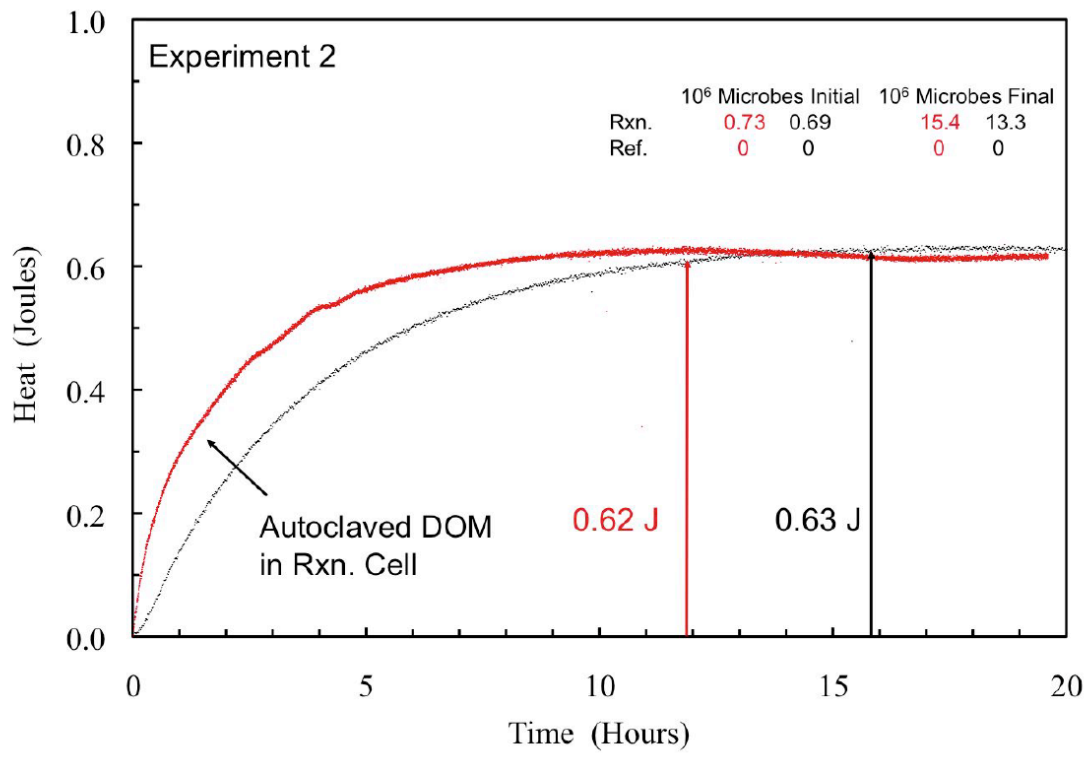


637  
 638  
 639  
 640

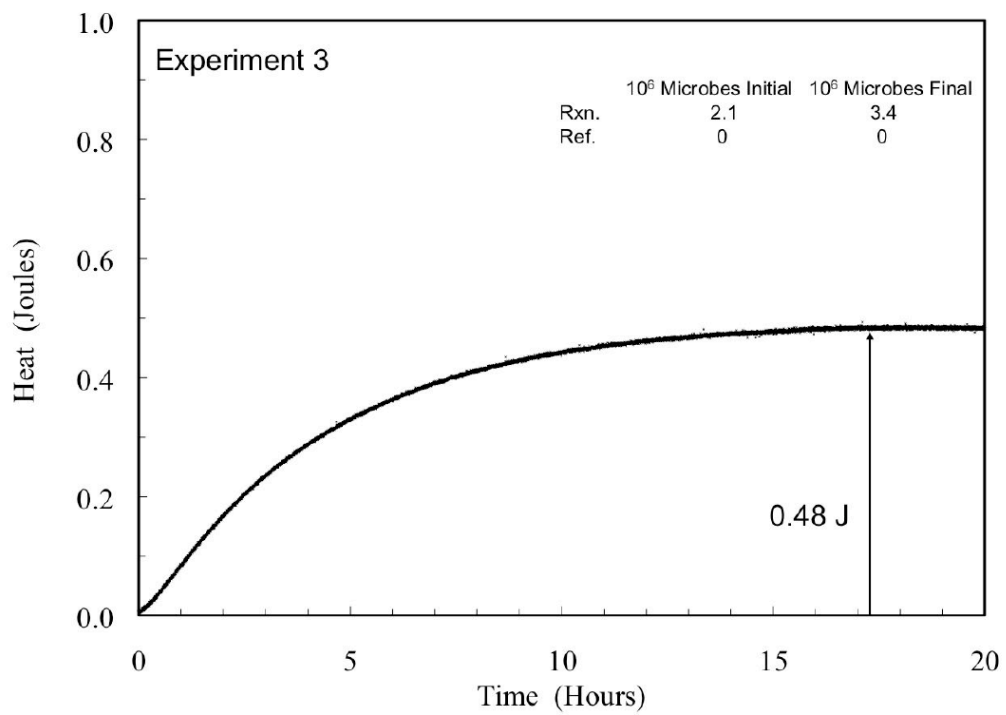
Fig 3



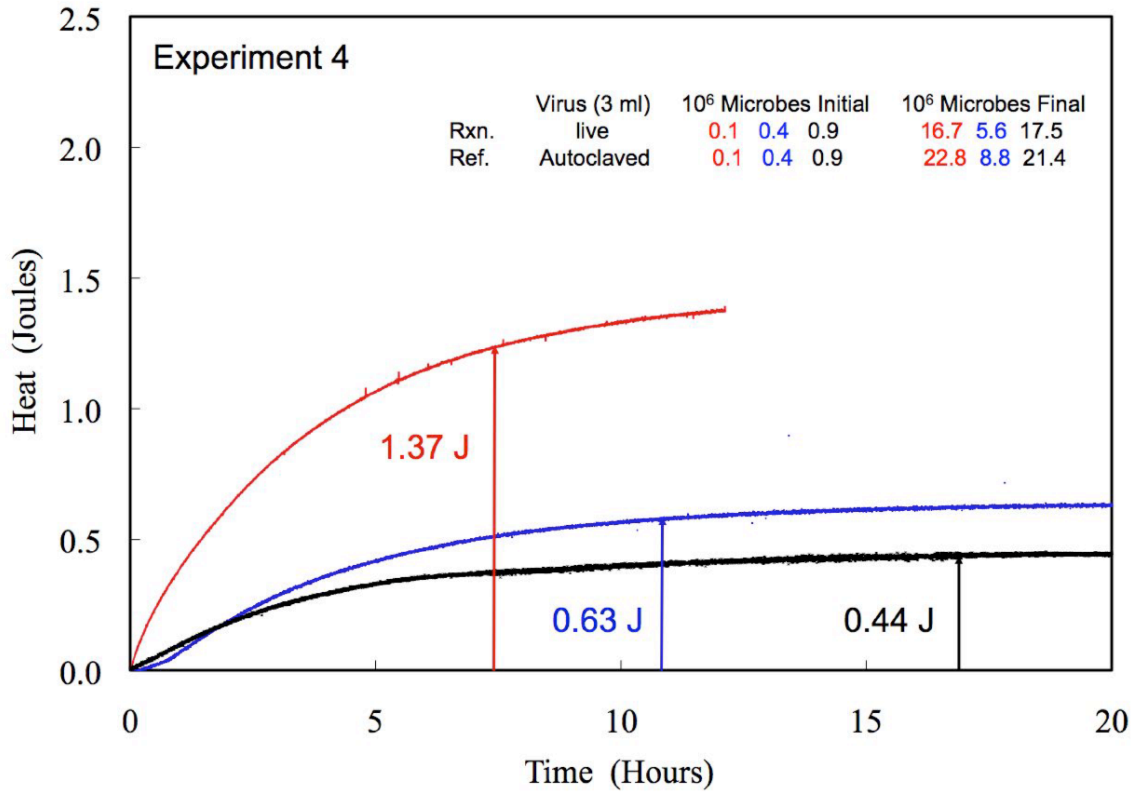
640  
641 Fig 4  
642



642  
643 Fig 5  
644



644  
 645 Fig 6  
 646



646  
 647 Fig 7  
 648